



THE INTERNATIONAL  
ENCYCLOPEDIA OF  
GEOGRAPHY

### Weathering processes and landforms

Journal:	<i>The International Encyclopedia of Geography: People, the Earth, Environment, and Technology</i>
Manuscript ID:	IEGE-13-0079.R1
Wiley - Manuscript type:	Entry
Date Submitted by the Author:	n/a
Complete List of Authors:	Dorn, Ronald Thompson, Tyler
Keywords:	climate / landform / vegetation history, geomorphology, landforms, scale, soils
Free Text Keywords:	
Abstract:	

SCHOLARONE™  
Manuscripts

Only

## **Weathering processes and landforms**

**Tyler J. Thompson**

*Arizona State University*

tjthomp9@asu.edu

and

**Ronald I. Dorn**

*Arizona State University*

ronald.dorn@asu.edu

Corresponding Author

### **Word Count (2055 words)**

[Includes Main Text, SEE ALSO: (cross-references), References and Further Readings.]

### **Abstract**

Rock-decay processes operating at the nanoscale and micron scale generate spectacular landforms that spike the curiosity of the general public and scholars alike. Tafoni holes in rock faces, meter-thick slabs of granite from the release of pressure, tors consisting of granitic boulders that pile up as decayed granite sand erodes away, limestone tower remnants left behind as thick carbonate deposits dissolve in the humid tropics, and many other bare-rock forms exemplify links between landforms and the processes that led to those forms.

### **Main Text**

This entry relates the appearance of bare-rock landforms to the processes of rock decay. [We use the term ‘rock decay’ rather than ‘weathering’ throughout this entry, because ‘weathering’ no longer functions as a useful scientific term (Hall et al. 2012), even though it is still widely used]. We start by introducing the topic by presenting a few classic examples connecting form to process, followed by an explanation of why bare-rock landforms occur. Then, case studies illustrate how the appearance of bare-rock landforms relates to rock decay. The last section details the importance of scale in rock decay.

Figure 1 compiles a few classic landforms often taught in introductory physical geography. In these classes, tafoni (1A) are typically linked with salt precipitation. Pressure release shells — sometimes incorrectly called exfoliation — form when enough overlying rock material erodes away to result in the formation of meter-thick shells (1B). Wildfire suddenly heats the water in the outer shell of a rock enough to spall scales off boulders (1C). Erosion of grussified granite exposes core stones that pile into tors (1D). Accumulation of silica, manganese and iron inside of weathering rinds results in case hardening (1F). Root growth exerts sufficient pressure to open pre-existing fractures (1G). All of these examples occur in sites where soil does not cover bare rock.

The fundamental difference between landforms of mostly bare rock (Figure 1) — the focus of this entry — and landforms covered with soil and regolith derives from an imbalance between the rate at which rock decay produces rock fragments ( $P_r$ ) and the rate of transport of these rock fragments ( $T_r$ ). Bare-rock slopes occur in deserts where  $T_r > P_r$  — stripping the rock of its cover of particles. In contrast, soil- and regolith-covered slopes occur in wetter areas where  $T_r < P_r$  — and plants play a key role of holding produced particles in place. A key determinant in whether landscapes are soil-covered or consist of a lot of bare rock is the rate at which rocks decay and soil is produced to cover the bare rock. This entry focuses on locations where soil production has not outpaced mass wasting, resulting in the exposure of rock.

**Case study 1: Petroglyphs and Rock Decay.** Petroglyph rock art panels display a wide range of forms linked to rock decay (Dorn et al. 2008). Figure 2 illustrates seven of these forms generated by different decay processes: (A) the splintering form of subparallel mm-scale cracks (Dorn et al. 2013); (B) spalling of cm-thick scales; (C) tafoni growth; (D) block separation along opening joints; (E) lithobiont-enhanced decay (Viles 1995); (F) weaknesses along bedding planes; and (G) salt precipitation resulting in the flaking a petroglyph panel face.

Microclimatic control and mineral assemblage permits communities of various epilithic lichens (Figure 2E) and microorganisms to inhabit the area between the surface and weathering front of the rock (Viles 1995). The acids generated by bacteria include citric, oxalic, nitric, sulphuric acid, and others. These acids accelerate dissolution rates of minerals. Where these microorganisms live within the substrate (whether on the surface, in rock fractures, tunnels, or pores) may impact the resultant decay. For example, ivy overhanging historic buildings can cause deterioration through exploiting fractures (root wedging), but may also moderate the microclimate of the wall reducing thermal stresses. Lichens also moderate the thermal stresses on blocks by storing moisture in their thallus and protecting the surface from temperature changes. Contrasting with these instances of bioprotection, chemical decay rates on olivine were shown to be greater underneath lichens due the combined effects of higher moisture retention and the secretion of organic acids (Brady et al. 1999).

Figure 3 illustrates the complexity of decay processes that can result in the flaking of a sandstone surface. First, a joint fracture opens slightly, allowing water movement and accumulation of silica glaze along the joint walls. Second, the overlying block erodes and exposes the joint face to the accumulation of rock varnish and iron film rock coatings. Third, the silica, iron and manganese in these coatings dissolve and remobilize into the underlying sandstone. This case hardens the outer shell of the sandstone, but it also inhibits water from flowing out of the rock; the case hardening thus acts as a ‘dam’ that allows capillary accumulate underneath the case hardening. Eventually, enough decay takes place underneath the case hardening to reach the point where the surface flakes away.

**Case study 2: Limestone in different environments.** Limestone dissolution typically proceeds along the lines of the chemical reaction:  $\text{CaCO}_3 + \text{CO}_2 + \text{H}_2\text{O} \rightarrow$

$\text{Ca}^{2+} + 2\text{HCO}_3^-$ , leading to the basic karst landforms of sinkholes, caves, and karren (White 1990) that occur in a wide variety of terrestrial environments. Consider the small-sized features such as flutes (Figure 3A), runnels (Figure 3C and 3D), slabs called clints separated deep fissures called grikes (Figure 3B). Karren occurs on bare surfaces in virtually all climatic settings. Substantial differences, however, do occur in the larger karst landforms found in drylands and the wet tropics. Stone forests (Figure 3D) and tower karst (Figure 3E) are forms that develop in the wet tropics, even if climatic changes can sometimes shift them into other environments. In contrast, arid and semi-arid regions tend to have only minimal development of relief associated with dissolution (e.g. deep sinkholes, deep valleys between towers and forest pinnacles). Arid and semi-arid limestone tends to stand out as higher relief relatively resistant to erosion, such as the cliff-forming Kaibab limestone of Arizona (Figure 1F) and anticlines in Iran (Figure 1G). The reason for the tendency of dryland limestone to be more resistant to dissolution clearly relates to the abundance of moisture and biotic acids that enhance dissolution rates. s

Scale cannot be ignored in the study of rock decay. Understanding forms at different scales — from individual grains to the scale of outcrops — is of critical importance in diagnosing the current susceptibility of rock-face features to erosion and therefore near-term stability. The system of the Rock Art Stability Index (RASI) (Dorn et al. 2008) illustrates the concurrent decay and erosion across the range of visible scales. For example in Figures 2G and 3, varnished rock surfaces displays scaling (erosion of centimeter-scale clasts) along the fringes of the varnish, while the weathering rind erodes granularly beneath the case-hardened surface. Additionally, detached blocks are subject to undercutting through block orientation in rock falls (Figure 2D). The idea of RASI rests in analyzing current processes and evidence of past processes that influence the threat of erosion to rocks, allowing field scientists to contribute to rock art conservation.

However, connecting processes at the finest scales to the forms seen in the field is both difficult and rarely considered. Consider form of splintering (Figure 2A). The splintering form resembles the pages of a book that went through a cycle of wetting and drying. At the hand-sample scale (Figure 5A), splintering appears to correspond with the development of aligned micron-scale fractures that carry capillary water. Then, at the micron-scale (Figure 5B) the fractures transporting capillary water align with nanoscale (Figure 5C) fractures. When these fractures do not align all the way down to the nanoscale, the splintering form does not occur (Dorn et al. 2013).

Landforms generated through rock decay processes are not restricted to any particular scale (Figure 6), but the scale at which a process operates is very important. The new frontier in rock decay studies rests at the nanoscale, where research has been slow to link across scales (Dorn et al. 2013). Nanoscale formation of rock coatings, such as silica glaze (Figure 6A), influence weathering rind and case hardening formation at the micron scale (Figure 6C). At micron scales, for example, weathering processes may dissolve (Figure 6F) and weaken the boundaries between mineral grains (Figure 6B). The cumulative effect of these minute processes may lead to patterns of granular disintegration on the stone (Figures 6D and 2E), the coating of slopes with salt (Figure 6), and the production of materials that generate alluvial fans (Figure 6H). The environment, be it the microclimate under a boulder, the soil accumulation within a rock fracture,

landscape geochemistry, or broad-area precipitation patterns, sets the bounds of rock decay and erosive interaction for the landform.

The ever-changing balance between rock decay processes and erosion generates the great variety of landscapes seen on Earth's surface. The forms seen in bare-rock landscapes reflect most closely rock decay, since erosion rates far exceed decay rates in these settings. Forms seen in the field result when decay proceeds far enough to result in detachment. Thus, in some settings, geological processes can control mineral compositions and textures that in turn help define chemical decay rates. In other settings, tectonic histories and material properties govern joint density and orientations, thus providing avenues for solution processes between joint walls and planes of future mass wasting failure. Organisms can play both protective and accelerative roles. Rock decay across scales ultimately sculpts landforms by generating points, planes, or zones of relative physical strength or weakness that are then exploited by agents of detachment and then transport.

**SEE ALSO:**

Fluvial erosional processes and landforms  
 Karst processes and landforms  
 Mass Movement processes and landforms  
 Periglacial processes and landforms  
 Tropical Geomorphology

**Key Words**

climate/landform/vegetation history  
 geomorphology  
 landforms  
 scale  
 soils

**References**

- Brady, P. V., R. I. Dorn, A. J. Brazel, J. Clark, R. B. Moore and T. Glidewell. 1999. "Direct measurement of the combined effects of lichen, rainfall, and temperature on silicate weathering." *Geochimica et Cosmochimica Acta*, 63: 3293-3300.
- Dorn, R. I., S. J. Gordon, D. Krinsley and K. Langworthy. 2013. "Nanoscale: Mineral weathering boundary." In *Treatise on Geomorphology*, Vol. 4, edited by G. A. Pope, 44-69. San Diego: Academic Press.
- Dorn, R. I., D. S. Whitley, N. C. Cervený, S. J. Gordon, C. Allen and E. Gutbrod. 2008. "The rock art stability index: A new strategy for maximizing the sustainability of rock art as a heritage resource." *Heritage Management*, 1: 35-70.
- Hall, K., C. E. Thorn and A. Sumner. 2012. "On the persistence of 'weathering'." *Geomorphology*, 149-150: 1-10.
- Viles, H. A. 1995. "Ecological perspectives on rock surface weathering: towards a conceptual model." *Geomorphology*, 13: 21-35.

White, W. B. 1990. "Surface and near-surface karst landforms." Geological Society of America Special Paper, 252: 157-176.

### Further Readings

- Carter, N. E. A. and H. A. Viles. 2003. "Experimental investigations into the interactions between moisture, rock surface temperatures and an epilithic lichen cover in the bioprotection of limestone." *Building and Environment*, 38: 1225-1234.
- Gilbert, G. K. 1877. *Geology of the Henry Mountains*. Washington D.C.: U.S. Geological and Geographical Survey.
- Linton, D. L. 1955. "The problem of tors." *The Geographical Journal*, 121: 470-481+487.
- Mol, L. and H. Viles. 2012. "The role of rock surface hardness and internal moisture in tafoni development in sandstone." *Earth Surface Processes and Landforms*, 37: 301 - 314.
- Mottershead, D. N., B. Bailey, P. Collier and R. J. Inkpen. 2003. "Identification and quantification of weathering by plant roots." *Building and Environment*, 38: 1235-1241.
- Navarre-Sitchler, A. and S. Brantley. 2007. "Basalt weathering across scales." *Earth and Planetary Science Letters*, 261: 321-334.
- Smith, B. J. 2009. "Weathering processes and forms." In *Geomorphology of Desert Environments*, 2nd edition, edited by A. J. Parsons and A. D. Abrahams, 69-100. Amsterdam: Springer.
- Turkington, A. V. and T. R. Paradise. 2005. "Sandstone weathering: a century of research and innovation." *Geomorphology*, 67: 229–253.
- Viles, H. A. 2011. "Microbial geomorphology: a neglected link between life and landscape." *Geomorphology*, 157: 6-16.
- Zhang, Z. 1980. "Karst types in China." *GeoJournal*, 4: 541-570.

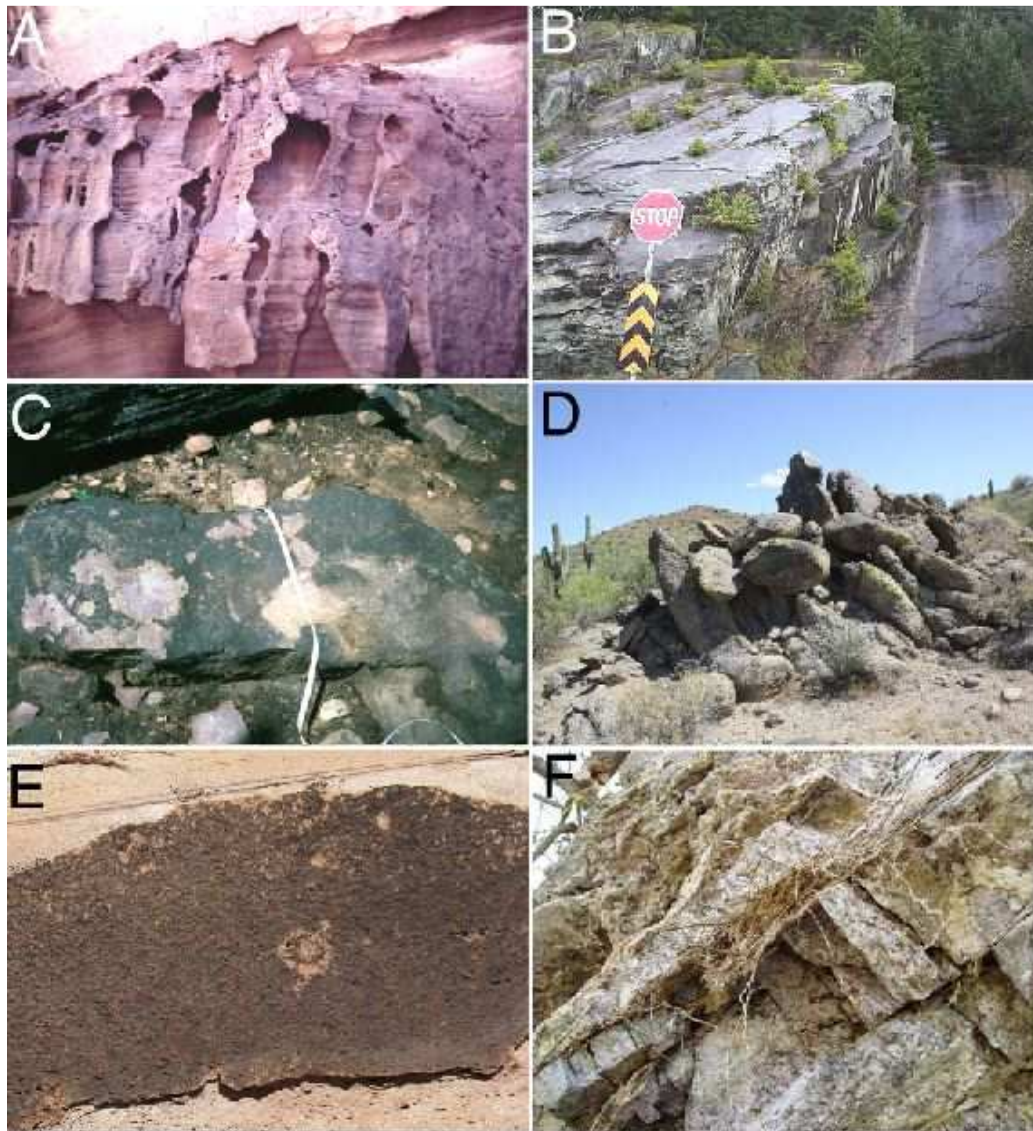


Figure 1. Classic forms associated with rock decay: (A) tafoni in sandstone at Timna, Negev Desert; (B) pressure release shells in granodiorite, British Columbia; (C) scaling of diorite from a wildfire, Arizona; (D) tor of granite, Sonoran Desert in Arizona; (E) case hardening of sandstone at Petrified Forest National Park in Arizona; (F) root pressure widening fractures in gneiss, Sonoran Desert, Arizona. Image widths approximately 3 m, 12 m, 2 m, 8 m, 0.5 m, 0.2 m for A-F respectively

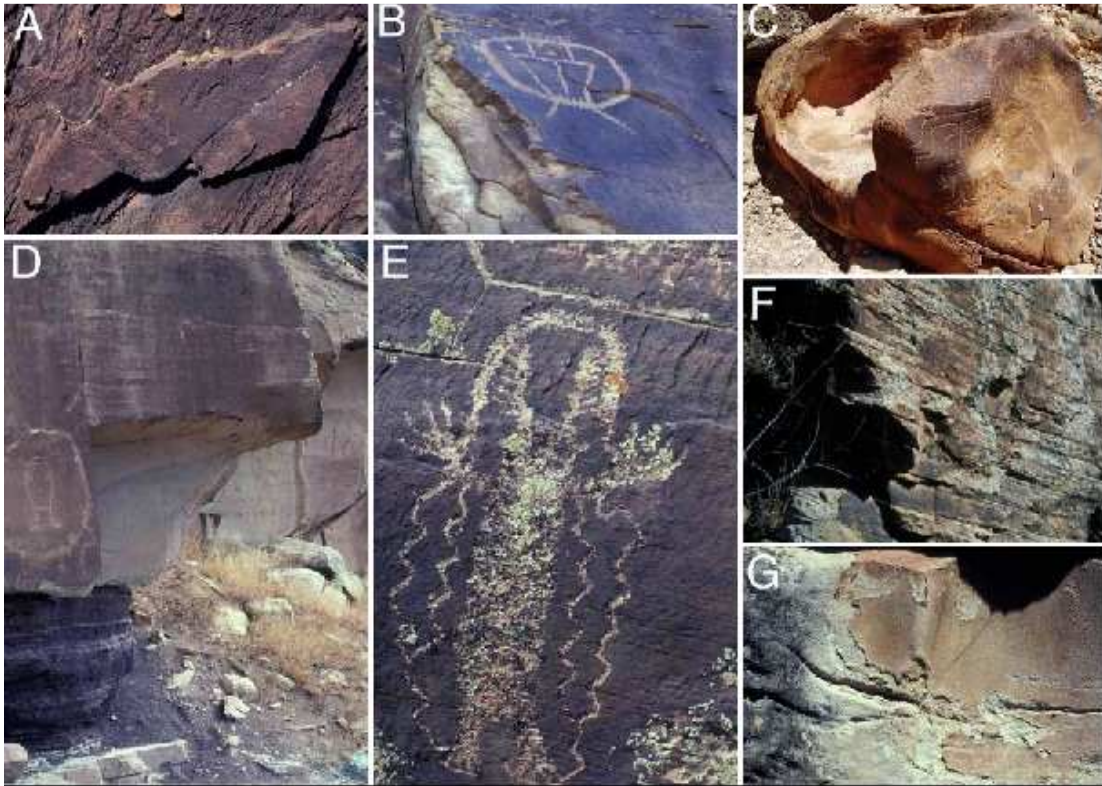


Figure 2 A variety of different processes degrade rock surfaces, illustrated here for sites with petroglyphs: (A) the splintering process on silicified dolomite, South Australia (B) spalling of joints in sandstone, Utah (C) tafoni formation through dissolution of grain-cementing agents in sandstone, Arizona (D) spalling of joints opened by dirt cracking and calcrete wedging, Utah (E) lithobiont-related crumbly disintegration of sandstone, Utah; (F) enhanced granular disintegration associated with joints that align with bedding planes in sandstone, Arizona; and (G) salt precipitation enhancing flaking of sandstone, Wyoming.

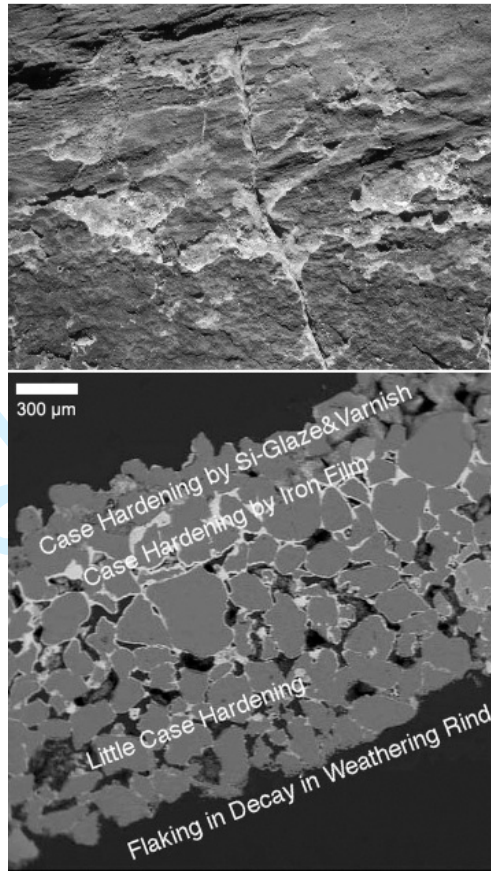


Figure 3. Sandstone surface at Whoopup Canyon, Black Hills, Wyoming (width of upper image about 30 cm) has case hardened due to the accumulation silica glaze, iron, and rock varnish in the pores in the outer millimeter of the rock. This then case hardening acted as a dam to store water underneath the case hardening, which dissolved the silica cement and enhanced detachment of the millimeter-scale flake. The lower backscattered electron image shows pores as black, the silica of the quartz grains as gray, and metal-rich areas as bright white.

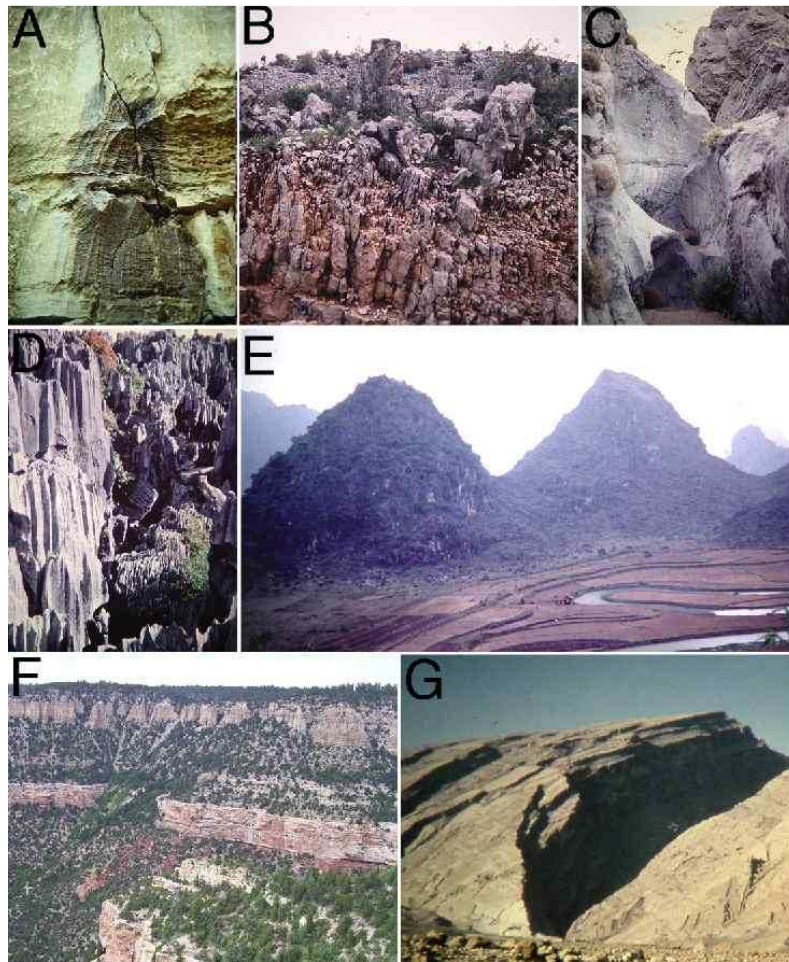
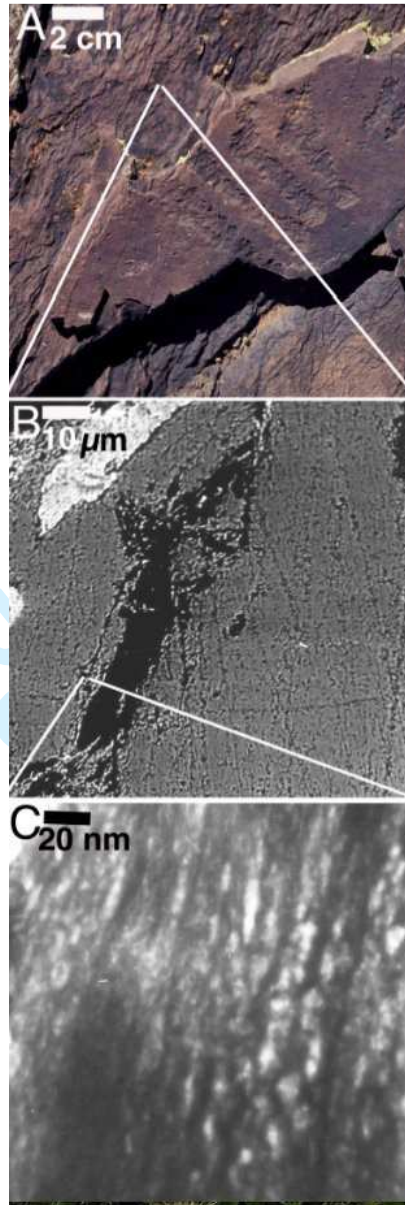


Figure 4. Limestone karst dissolution landforms in different environmental settings: (A) flutes in semi-arid Trans-Pecos Texas; (B) clints and grikes in semi-arid northern Israel; (C) large flute associated with rare fluvial discharge in arid drainage basin, eastern California; (D) stone forest in China; (E) tower karst in China; (F) cuesta face, northern Arizona; (G) anticline, Iran.

Figure 5. The weathering form of splintering of a silicified dolomite, South Australia (A) at the hand-sample scale (B) a micron-scale backscattered electron microscope image (C) a nanoscale-scale transmission electron microscope image.



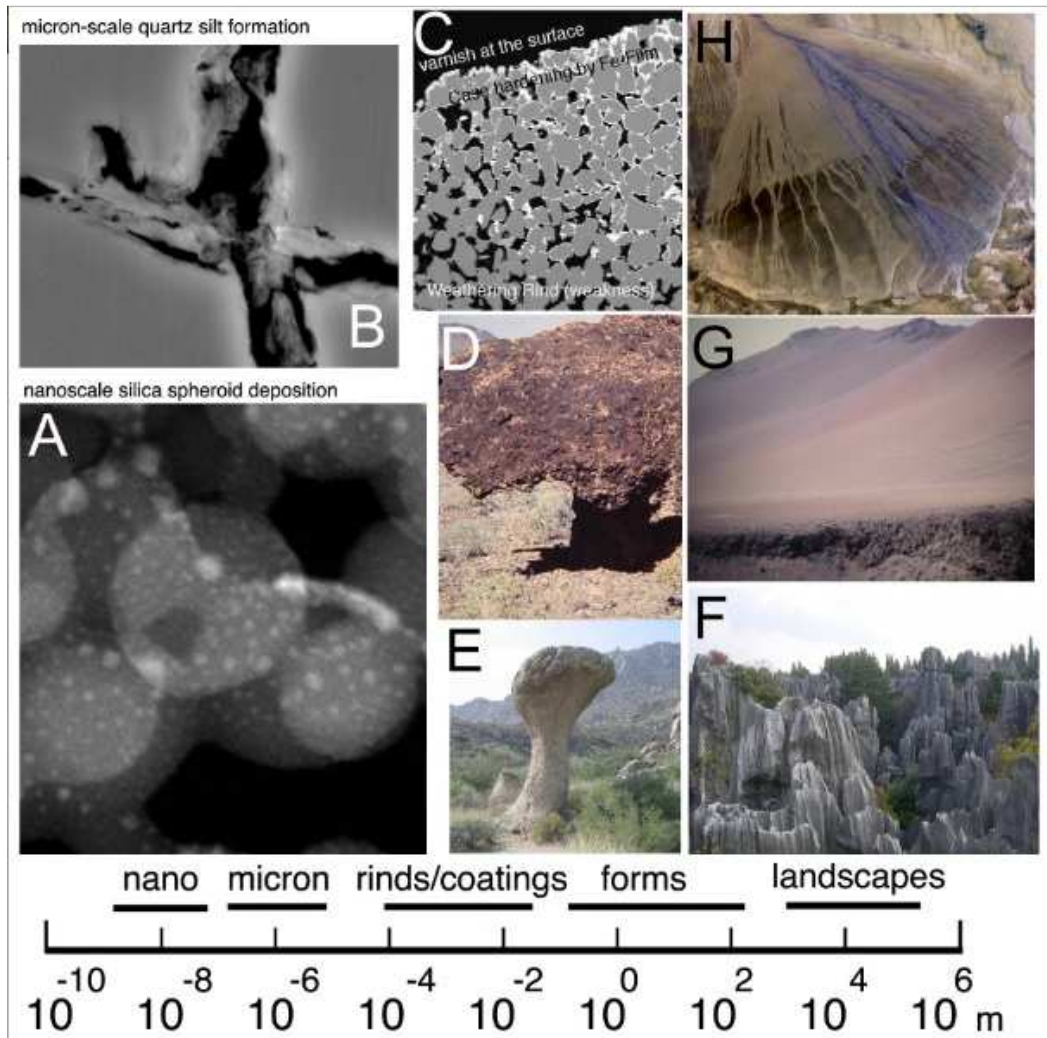


Figure 6. Visualization of nanoscale decay placed within broader spatial scales of rock decay phenomenon. Examples presented from nano to landscape scales are: (A) nanoscale silica spheroids a few tens of nm across from silica glaze in Tibet (high-resolution transmission electron microscopy (HRTEM) image); (B) micron-scale silt formation from quartz weathering in Arizona (back-scattered electron (BSE) image); (C) millimeter to centimeter-scale rock coatings and weathering rinds illustrated from Wyoming (BSE image) and (D) Death Valley (case hardened rock shelter); (E) meter-scale forms of a mushroom rock, Arizona and (F) limestone karst stone forest, Kunming, China; and (G) kilometer-scale landscapes of a salt-encrusted marine terrace, Peru, and (H) varnish-coated alluvial fan, western China, courtesy of NASA.

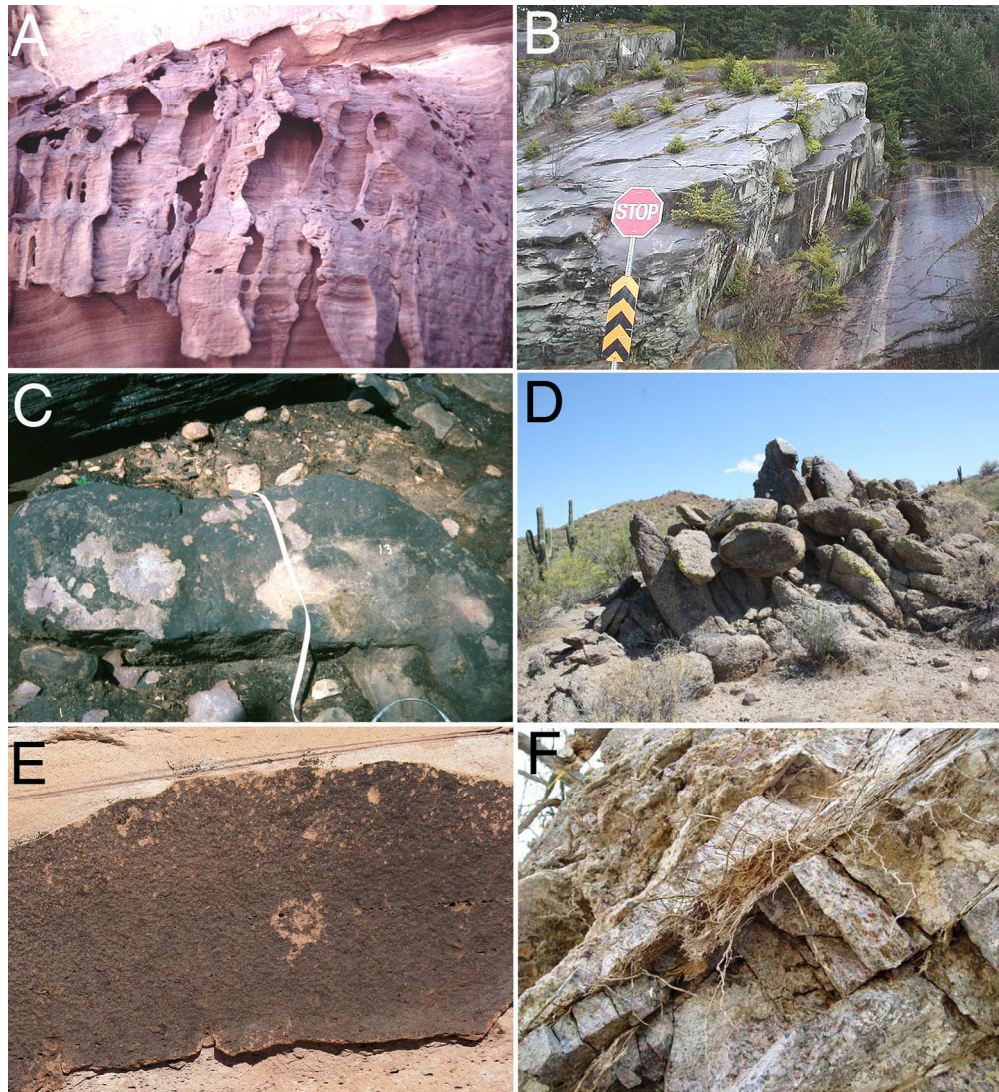


Figure 1. Classic forms associated with rock decay: (A) tafoni in sandstone at Timna, Negev Desert; (B) pressure release shells in granodiorite, British Columbia; (C) scaling of diorite from a wildfire, Arizona; (D) tor of granite, Sonoran Desert in Arizona; (E) case hardening of sandstone at Petrified Forest National Park in Arizona; (F) root pressure widening fractures in gneiss, Sonoran Desert, Arizona. Image widths approximately 3 m, 12 m, 2 m, 8 m, 0.5 m, 0.2 m for A-F respectively  
145x158mm (300 x 300 DPI)

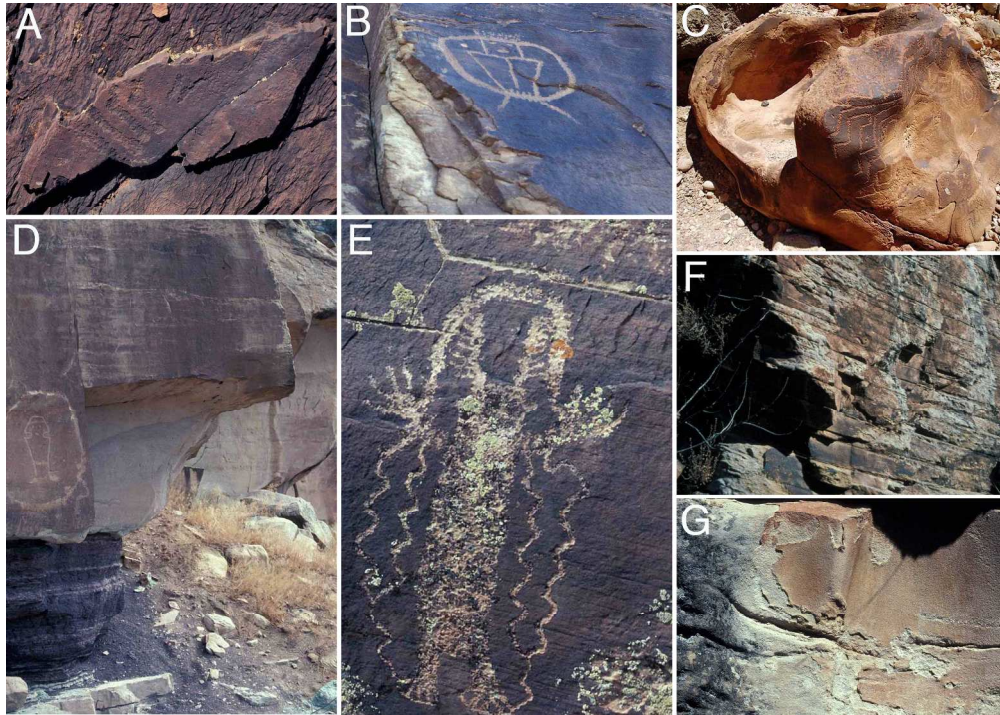


Figure 2 A variety of different processes degrade rock surfaces, illustrated here for sites with petroglyphs: (A) the splintering process on silicified dolomite, South Australia (B) spalling of joints in sandstone, Utah (C) tafoni formation through dissolution of grain-cementing agents in sandstone, Arizona (D) spalling of joints opened by dirt cracking and calcrete wedging, Utah (E) lithobiont-related crumbly disintegration of sandstone, Utah; (F) enhanced granular disintegration associated with joints that align with bedding planes in sandstone, Arizona; and (G) salt precipitation enhancing flaking of sandstone, Wyoming.  
307x218mm (300 x 300 DPI)

Only

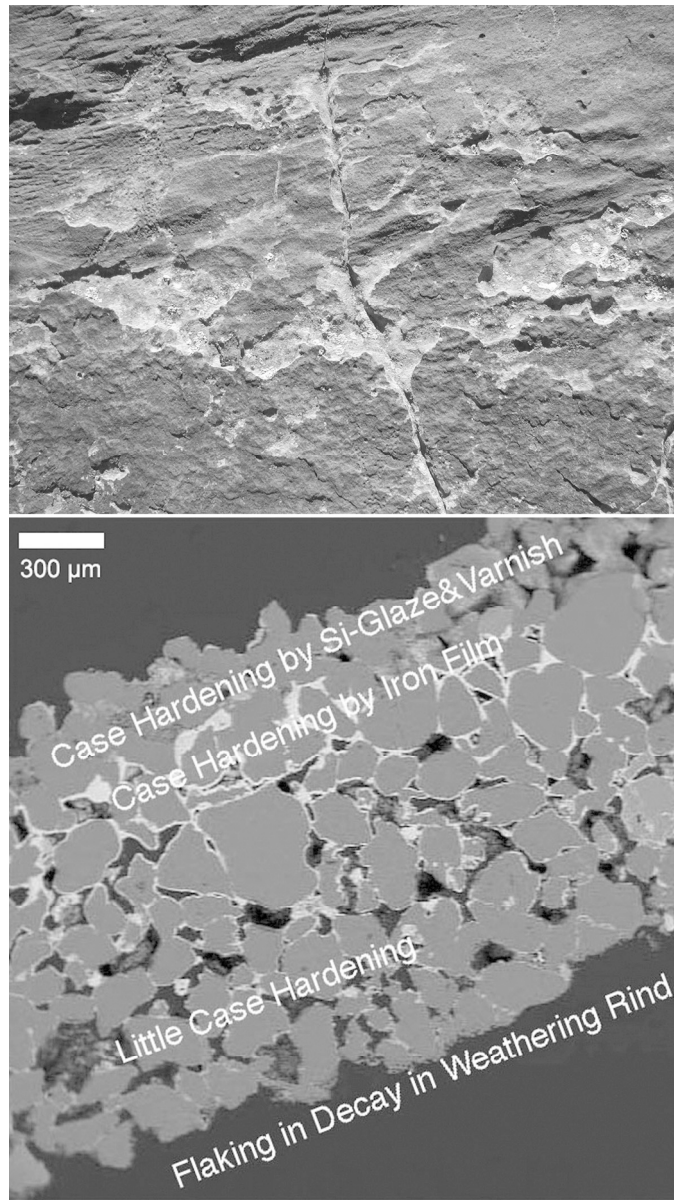


Figure 3. Sandstone surface at Whoopup Canyon, Black Hills, Wyoming (width of upper image about 30 cm) has case hardened due to the accumulation silica glaze, iron, and rock varnish in the pores in the outer millimeter of the rock. This then case hardening acted as a dam to store water underneath the case hardening, which dissolved the silica cement and enhanced detachment of the millimeter-scale flake. The lower backscattered electron image shows pores as black, the silica of the quartz grains as gray, and metal-rich areas as bright white.  
101x179mm (300 x 300 DPI)

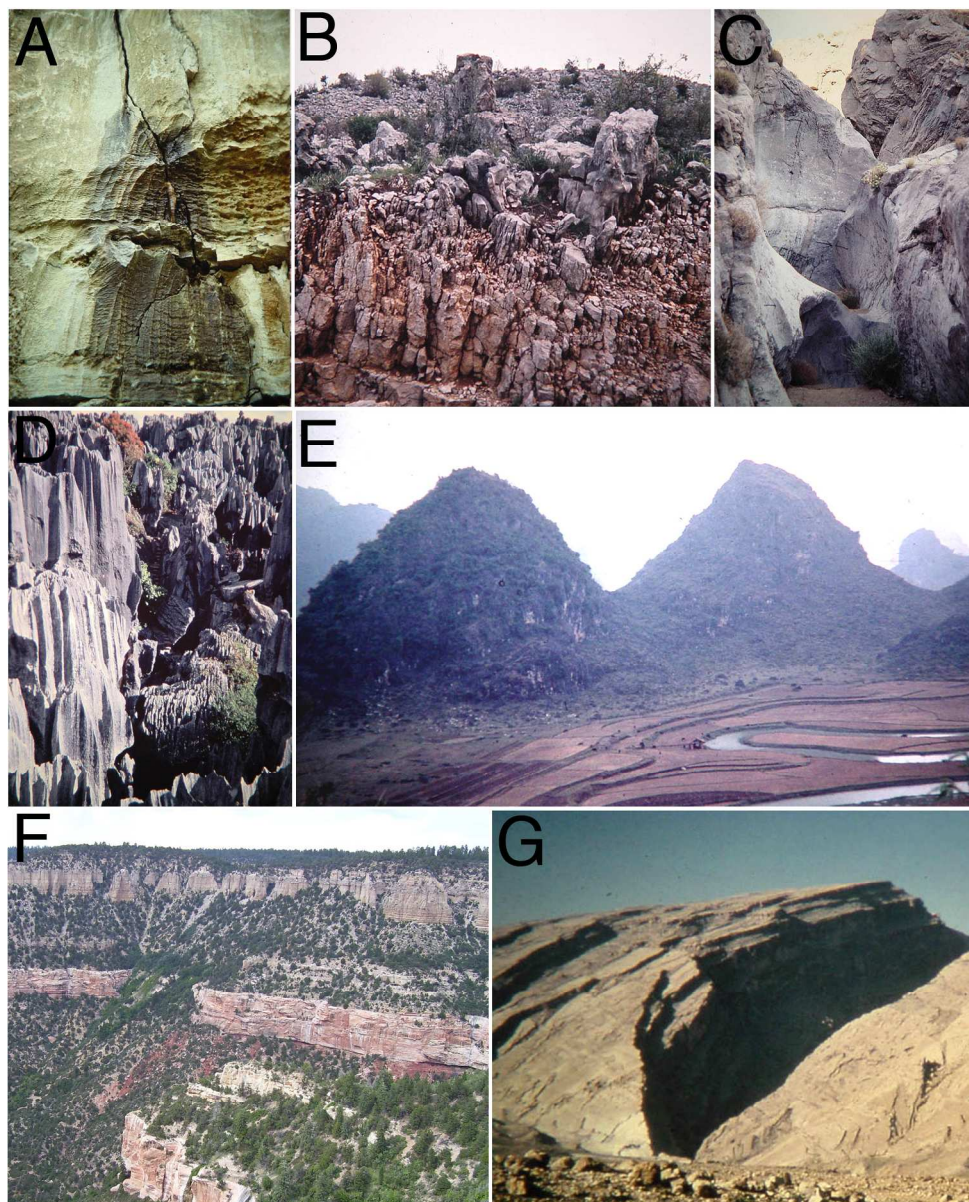


Figure 4. Limestone karst dissolution landforms in different environmental settings: (A) flutes in semi-arid Trans-Pecos Texas; (B) clints and grikes in semi-arid northern Israel; (C) large flute associated with rare fluvial discharge in arid drainage basin, eastern California; (D) stone forest in China; (E) tower karst in China; (F) cuesta face, northern Arizona; (G) anticline, Iran.

186x230mm (300 x 300 DPI)

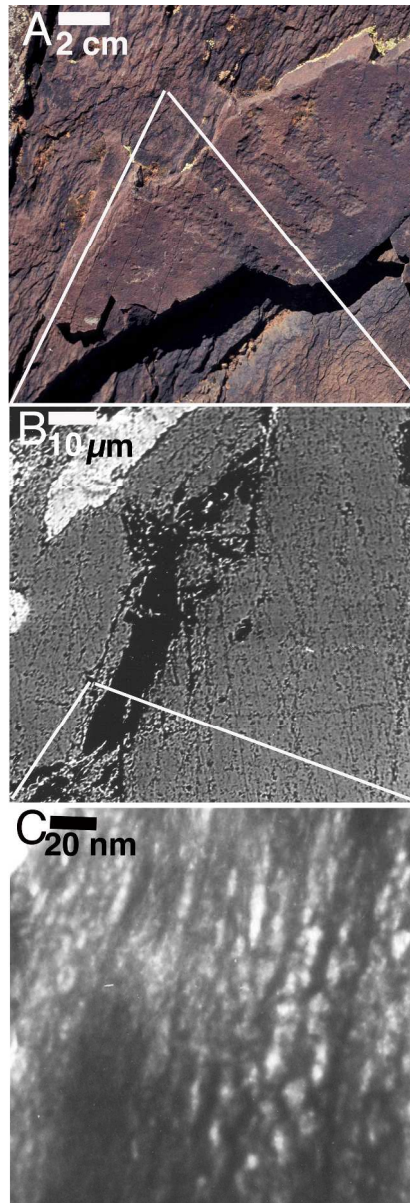


Figure 5. The weathering form of splintering of a silicified dolomite, South Australia (A) at the hand-sample scale (B) a micron-scale backscattered electron microscope image (C) a nanoscale-scale transmission electron microscope image.  
125x367mm (300 x 300 DPI)

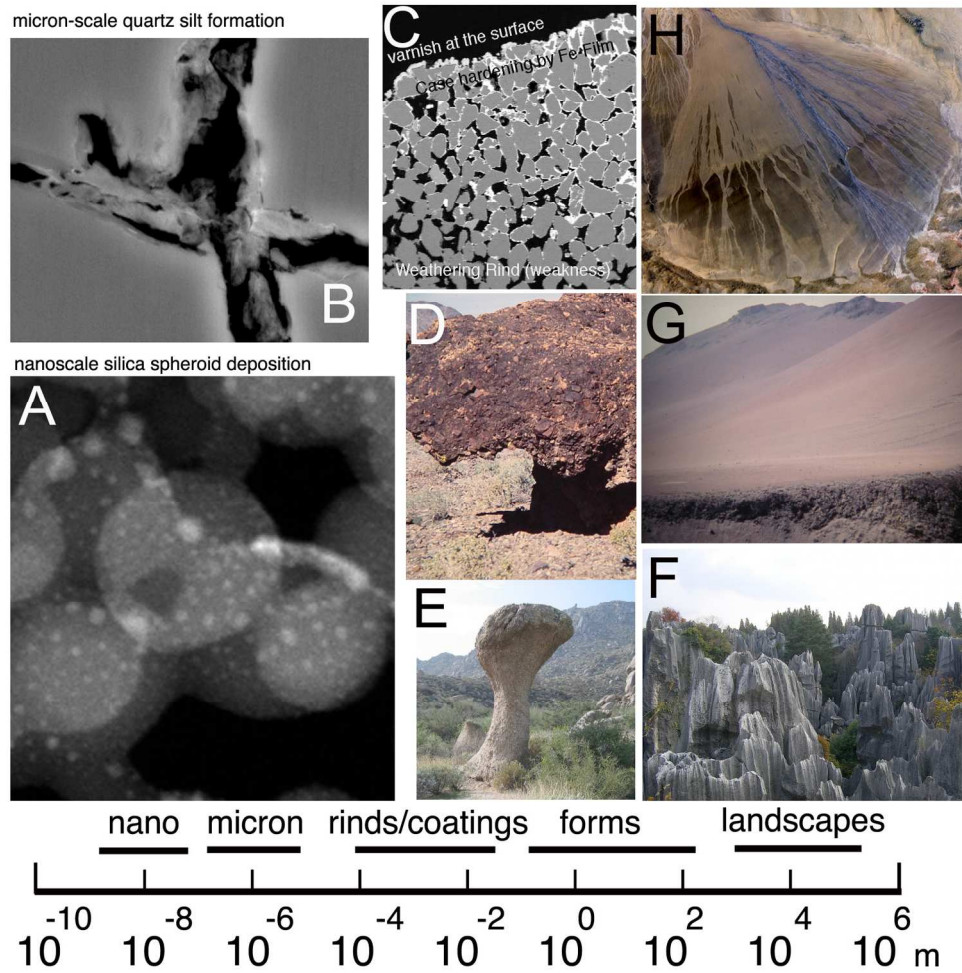


Figure 6. Visualization of nanoscale decay placed within broader spatial scales of rock decay phenomenon. Examples presented from nano to landscape scales are: (A) nanoscale silica spheroids a few tens of nm across from silica glaze in Tibet (high-resolution transmission electron microscopy (HRTEM) image); (B) micron-scale silt formation from quartz weathering in Arizona (back-scattered electron (BSE) image); (C) millimeter to centimeter-scale rock coatings and weathering rinds illustrated from Wyoming (BSE image) and (D) Death Valley (case hardened rock shelter); (E) meter-scale forms of a mushroom rock, Arizona and (F) limestone karst stone forest, Kunming, China; and (G) kilometer-scale landscapes of a salt-encrusted marine terrace, Peru, and (H) varnish-coated alluvial fan, western China, courtesy of NASA.  
152x152mm (300 x 300 DPI)